

RESEARCH ARTICLE

# Chromosomal diversity and molecular divergence among three undescribed species of *Neacomys* (Rodentia, Sigmodontinae) separated by Amazonian rivers

Willam Oliveira Da Silva<sup>1</sup>, Julio Cesar Pieczarka<sup>1</sup>, Malcolm Andrew Ferguson-Smith<sup>2</sup>, Patricia Caroline Mary O'Brien<sup>2</sup>, Ana Cristina Mendes-Oliveira<sup>3</sup>, Iracilda Sampaio<sup>4</sup>, Jeferson Carneiro<sup>4</sup>, Cleusa Yoshiko Nagamachi<sup>1\*</sup>

**1** Centro de Estudos Avançados da Biodiversidade, Laboratório de Citogenética, Instituto de Ciências Biológicas, Universidade Federal do Pará (UFPA), Belém, Brasil, **2** Cambridge Resource Centre for Comparative Genomics, Department of Veterinary Medicine, University of Cambridge, Cambridge, United Kingdom, **3** Laboratório de Zoologia e Ecologia de Vertebrados, ICB, Universidade Federal do Pará (UFPA), Pará, Brasil, **4** Laboratório de Genética e Biologia Molecular, Universidade Federal do Pará, Campus Universitário de Bragança, Pará, Brasil

\* [cleusanagamachi@gmail.com](mailto:cleusanagamachi@gmail.com), [cleusanagamachi@pq.cnpq.br](mailto:cleusanagamachi@pq.cnpq.br)



**OPEN ACCESS**

**Citation:** Oliveira Da Silva W, Pieczarka JC, Ferguson-Smith MA, O'Brien PCM, Mendes-Oliveira AC, Sampaio I, et al. (2017) Chromosomal diversity and molecular divergence among three undescribed species of *Neacomys* (Rodentia, Sigmodontinae) separated by Amazonian rivers. PLoS ONE 12(8): e0182218. <https://doi.org/10.1371/journal.pone.0182218>

**Editor:** Tzen-Yuh Chiang, National Cheng Kung University, TAIWAN

**Received:** February 20, 2017

**Accepted:** July 15, 2017

**Published:** August 1, 2017

**Copyright:** © 2017 Oliveira Da Silva et al. This is an open access article distributed under the terms of the [Creative Commons Attribution License](https://creativecommons.org/licenses/by/4.0/), which permits unrestricted use, distribution, and reproduction in any medium, provided the original author and source are credited.

**Data Availability Statement:** Data are available from Genbank (molecular data; accession numbers included in S1 Table) or from the S1 Fig (cytogenetic data).

**Funding:** This work was funded by the Conselho Nacional de Desenvolvimento Científico e Tecnológico (CNPq) 552032/2010-7, the Fundação de Amparo à Pesquisa do Pará (FAPESPA) 007/2011 and 2010/110447, and the Coordenação de

## Abstract

The *Neacomys* genus (Rodentia, Sigmodontinae) is distributed in the Amazon region, with some species limited to a single endemic area, while others may occur more widely. The number of species within the genus and their geographical boundaries are not known accurately, due to their high genetic diversity and difficulties in taxonomic identification. In this work we collected *Neacomys* specimens from both banks of the Tapajós River in eastern Amazon, and studied them using chromosome painting with whole chromosome probes of *Hylaeamys megacephalus* (HME; Rodentia, Sigmodontinae), and molecular analysis using haplotypes of mitochondrial genes COI and Cytb. Chromosome painting shows that *Neacomys* sp. A (NSP-A, 2n = 58/FN = 68) and *Neacomys* sp. B (NSP-B, 2n = 54/FN = 66) differ by 11 fusion/fission events, one translocation, four pericentric inversions and four heterochromatin amplification events. Using haplotypes of the concatenated mitochondrial genes COI and Cyt b, *Neacomys* sp. (2n = 58/FN = 64 and 70) shows a mean divergence of 6.2% for *Neacomys* sp. A and 9.1% for *Neacomys* sp. B, while *Neacomys* sp. A and *Neacomys* sp. B presents a medium nucleotide divergence of 7.4%. Comparisons were made with other published *Neacomys* data. The Tapajós and Xingu Rivers act as geographic barriers that define the distribution of these *Neacomys* species. Furthermore, our HME probes reveal four synapomorphies for the *Neacomys* genus (associations HME 20/[13,22]/4, 6a/21, [9,10]/7b/[9,10] and 12/[16,17]) and demonstrate ancestral traits of the Oryzomyini tribe (HME 8a and 8b, 18 and 25) and Sigmodontinae subfamily (HME 15 and 24), which can be used as taxonomic markers for these groups.

Aperfeiçoamento de Pessoal de Nível Superior (CAPES) to CYN (Edital BIONORTE-CNPq, Proc 552032/2010-7; Edital BIONORTE-FAPESPA, ICAAF 007/2011; Edital Pró-Amazônia Proc 047/2012). This work was also supported by FAPESPA (Edital Vale – Proc 2010/110447) and the Banco Nacional de Desenvolvimento Econômico e Social – BNDES (Operação 2.318.697.0001) to JCP. This study is part of the Doctoral thesis of WOS in Genetic and Molecular Biology, under a CAPES Doctoral Scholarship vinculated on a project Pró-Amazônia (Proc. 047/2012) coordinated by CYN. CYN (308428/20013-7) and JCP (308401/2013-1) are grateful to CNPq for Productivity Grants. The funders had no role in study design, data collection and analysis, decision to publish, or preparation of the manuscript.

**Competing interests:** The authors have declared that no competing interests exist.

## Introduction

The Amazon is one of the richest biomes in terms of Brazilian mammalian species [1]. However, this biodiversity is not homogeneously distributed. Theories that consider ecologic, morphologic, chromosomal and/or molecular analysis performed with terrestrial vertebrate taxonomic groups have shown the occurrence of distinct biogeographic regions in the Amazon [2–4].

The large Amazonian rivers are suggested as major geographic barriers to species distribution in the region [3, 5, 6]. The Riverine Barrier Hypothesis was first proposed by Wallace [7] and reviewed by many authors [8, 9]. Silva et al. [5] recognize eight distinct endemic areas for Amazonian species limited by the major rivers: Belém, Guiana, Imeri, Inambari, Napo, Rondônia, Tapajós and Xingu. Each one of them has a distinct evolutionary history, with regard to species diversification.

Taxonomic studies in the Amazonian regions have been difficult because of overlapping characteristics between distinct species [10]. The taxonomy issue of rodents from the Sigmodontinae subfamily (Rodentia, Cricetidae) has been a problem, since this subfamily belongs to one of the most complex and diverse group of New World mammals [11, 12].

Recently, genetic strategies have helped to solve problems related to evolution and taxonomy, such as the comparative analysis of mitochondrial gene sequences of Cytochrome C Oxidase—subunit I (COI) and Cytochrome b (Cytb), frequently used for the comparison of species in the same genus or the same family [13]. Also, chromosome painting has been useful for karyotypic evolution studies based on cross-species chromosome homology [14, 15], but only 24 species from seven genera among the Sigmodontinae have been analyzed by this technique [16–23]. *Neacomys* has been one genus in which the understanding of karyotype evolution is complicated by the number of species, geographic boundaries and phylogenetic relationships.

The *Neacomys* genus Thomas, 1900 (Sigmodontinae, Oryzomyini) currently includes eight valid species with a known distribution in Central and South America, and only two species that do not occur in the Brazilian Amazon (*N. pictus* and *N. tenuipes*) [2, 24–28] (Table 1). However, the occurrence and geographic boundaries of the distribution of *Neacomys* species are poorly known, as are a large number of Amazon terrestrial mammalian taxa [2, 29].

**Table 1. Cytogenetic data available for *Neacomys* genus, with diploid number (2n) and autosomal fundamental number (FN).**

Species	2n	FN	References
<i>N. dubosti</i> Voss, Lunde, and Simmons, 2001	62	-	Voss et al. [25]
<i>N. dubosti</i> Voss, Lunde, and Simmons, 2001	64	68	Da Silva et al. [28]
<i>N. guianae</i> Thomas, 1905	56	-	Baker et al. [24]
<i>N. minutus</i> Patton, da Silva, and Malcolm, 2000	35–36	40	Patton et al. [29]
<i>N. musseri</i> Patton, da Silva, and Malcolm, 2000	34	64–68	Patton et al. [29]
<i>N. paracou</i> Voss, Lunde, and Simmons, 2001	56	-	Voss et al. [25]
<i>N. paracou</i> Voss, Lunde, and Simmons, 2001	56	62, 66	Da Silva et al. [28]
<i>Neacomys</i> sp.	58	64, 70	Da Silva et al. [28]
<i>N. spinosus</i> Thomas, 1882	64	68	Patton et al. [29]
<i>N. tenuipes</i> Thomas, 1900	56	-	Pérez-Zapata et al. (1996) <i>apud</i> Redi et al. [26]

<https://doi.org/10.1371/journal.pone.0182218.t001>

Cytogenetic studies of the genus *Neacomys* reveal variation in the diploid number from 34 to 64 and the fundamental number (FN) from 40 to 70 (Table 1). Recently Da Silva et al. [28] studied three *Neacomys* species and described five new karyotypes: one for *N. dubosti* ( $2n = 64/\text{FN} = 68$ ), two for *N. paracou* ( $2n = 56/\text{FN} = 62$  and  $66$ ) and two for *Neacomys* sp. ( $2n = 58/\text{FN} = 64$  and  $70$ ). Furthermore, the authors also generated a molecular phylogeny using *Cytb*, confirming the monophyly of *Neacomys* [2, 25, 30–32] and the status of *Neacomys* sp. as a previously undescribed species.

In order to test the Riverine Barrier Hypothesis, the present study compared *Neacomys* from different banks of Amazon rivers. We defined the karyotypes of two undescribed species of *Neacomys*, *Neacomys* sp. A (NSP-A,  $2n = 58/\text{FN} = 68$ ) and *Neacomys* sp. B (NSP-B,  $2n = 54/\text{FN} = 66$ ), collected from the right and left banks respectively, of the Tapajós River in Eastern Amazon. Whole chromosome probes of *Hylaeamys megacephalus* (HME) [20], were used to determine regions of chromosomal homology, and the mitochondrial genes COI and *Cytb* were used for molecular analysis. These results were compared with those from an undescribed species mentioned by da Silva et al. [28]. We present biogeographic inferences and discuss the chromosomal evolution of these taxa.

## Material and methods

Animals collected during this study were handled following procedures recommended by the American Society of Mammalogists. JCP has a permanent field permit, number 13248 from “Instituto Chico Mendes de Conservação da Biodiversidade”. The Cytogenetics Laboratory from UFPa has permit number 19/2003 from the Ministry of Environment for sample transport and permit 52/2003 for using the samples for research. The Ethics Committee (Comitê de Ética Animal da Universidade Federal do Pará) approved this research (Permit 68/2015). The rodents were maintained in the lab with food and water, free from stress, until their euthanasia using intraperitoneal injection of barbiturate (Pentobarbital, 120 mg/kg) after local anesthetic (lidocaine used topically).

We studied the karyotypes of nine specimens (five males and four females including one fetus) of *Neacomys* sp. A, collected from the right bank of the Tapajós River, in the Itaituba (Fig 1, localities 5, 6 and 8) and Jacareacanga municipalities (Fig 1, localities 7 and 9), Pará state, Brazil; seven specimens of *Neacomys* sp. B, three (one female and two males—one fetus) from the Itaituba municipality (Fig 1, locality 4) and four (three males and one female) from the Juruti municipality (Fig 1, locality 3), both from the left bank of the Tapajós River, Pará state, Brazil (S1 Table).

Samples were collected using Pitfall traps [33] and deposited at the mammal collection of Museu de Zoologia da Universidade Federal do Pará (UFPa), in Belém, Pará, Brazil. Chromosomal preparations were obtained from bone marrow [34] and by fibroblast cell culture made from two fetuses, established in the Centro de Estudos Avançados da Biodiversidade, Laboratório de Citogenética, Instituto de Ciências Biológicas, Universidade Federal do Pará, Belém, Pará, Brazil. G-banding and C-banding were performed following Sumner et al. [35] and Sumner [36], respectively. Fluorescent *in situ* Hybridization (FISH) studies were made using telomeric probes (All Telomere, ONCOR) and chromosome painting with whole chromosome probes of HME [20]. Twenty-one of the 24 probes of HME correspond to one HME chromosome pair, while three probes correspond to two pairs ([9,10]; [13,22]; [16,17]). Digital images were obtained by Nis-Elements software and Nikon H550S microscopy. Chromosome classification followed Levan et al. [37].

The map was made using QUANTUM-GIS (QGIS) program version 2.10.1. Database were obtained from DIVA and IBGE.

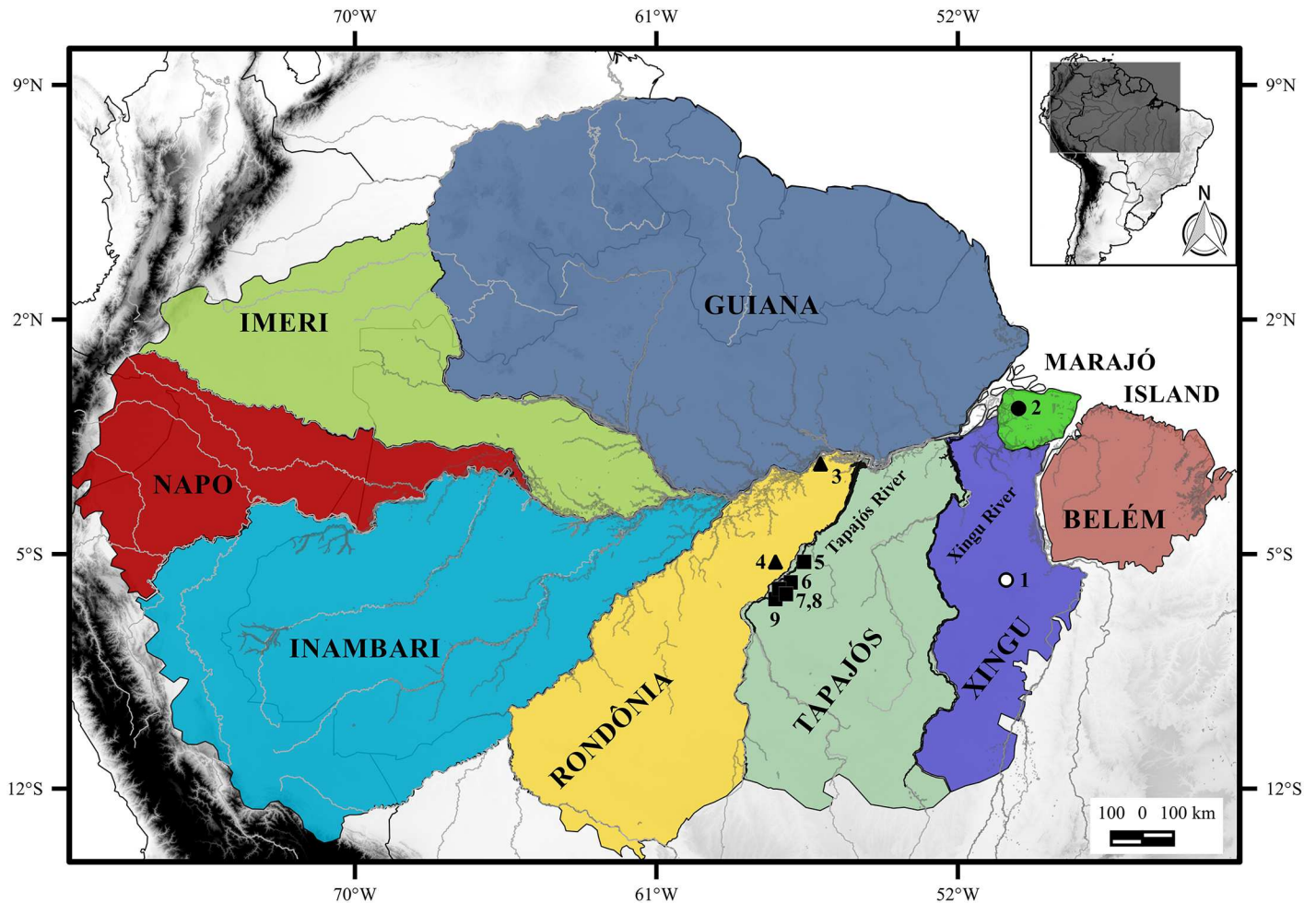


**Fig 1. Amazon endemic areas based on the distribution of terrestrial vertebrates [5].** Collection points of *Neacomys* sp. A (NSP-A; Black square), *Neacomys* sp. B (NSP-B; black triangle) and *Neacomys* sp. (white and black circle) [28]. Tapajós and Xingu Rivers are highlighted in black. The numbers refer to localities mentioned in S1 Table. (1) Marabá; (2) Chaves, Marajó island; (3) Juruti; (4, 5, 6 and 8) Itaituba; (7 and 9) Jacareacanga, all in Pará state, Brazil.

<https://doi.org/10.1371/journal.pone.0182218.g001>

We used sequences of 625 base pairs from 26 samples for Cytochrome C Oxidase—subunit I (COI), with 20 new sequences (*Neacomys* sp. A and *Neacomys* sp. B) and six sequences obtained from GenBank (S1 Table). For Cytochrome b (Cytb) we used sequences of 801 base pairs from 32 samples, with 18 new (*Neacomys* sp. A and *Neacomys* sp. B), and the others were kindly supplied by J.L. Patton (Museum of Vertebrate Zoology, Berkeley) or retrieved from GenBank (S1 Table). We included data from da Silva et al. [28] on an undescribed species (here mentioned as “*Neacomys* sp.”) found in Marabá and Marajó Island (Fig 1, places 1 and 2).

The DNA was extracted with Wizard<sup>®</sup> Genomic DNA Purification Kit (Promega, Madison, WI, USA). COI gene fragment amplification was made with the primers Fish F1 [5′ – TCAACCAACCACAAAGACATTGGC AC–3′] and Fish R1 [5′ – TAGACTTCTGGGTGGC CAAAGA ATCA–3′] [38], and Cytb was made with the primers MVZ-05 CGAAGCTTGATAT GAAAACCATCGTTG [38] and MVZ-16 AAATAGGAARTATCAYTCTGGTTTRAT [39].

The DNA sequencing used the Big Dye ABI PRISMTM Dye Terminator Cycle Sequencing kit, in the automated sequencer ABI 3500 (Applied Biosystems—Carlsbad, CA, USA).

The two markers were concatenated and phylogenetic analyzes were performed from haplotypes. The evolutionary model was generated by the software Kakusan v. 4–4.0.2015.01.23 [40], which selected GTR + GAMA as the most appropriate evolutionary model.

The genetic distance between taxa was estimated with Molecular Evolutionary Genetics Analysis—MEGA v. 6.0 software [41], recovering K2P model.

The phylogenetic reconstructions were made using both the maximum likelihood (ML) method, run in RaxML v. 8 [42] with 1000 bootstrap replicates and Bayesian inference (BI) as implemented in MrBayes v. 3.2.1 [43]. In MrBayes, the analysis of substitution model parameters was unlinked across partitions. Two independent runs were initiated simultaneously with four independent Markov-Chain Monte Carlo (MCMC) chains (one cold and three heated). The MCMC algorithm was based on 700,000 cycles (generations), sampled every 5,000 cycles, with 20% of the samples being discarded as burn-in. Convergence was assessed by comparing the two runs. The MCMC output was visualized and diagnosed in Tracer v. 1.6 [44]. The run was considered satisfactory when, for all traces, the Effective Sample Size (ESS) values were over 200. *Hylaeamys megacephalus*, *Oecomys rutilus*, *O. concolor*, *Deltamys* and *Thalpomys* were used as outgroup. All these species belong to the Sigmodontinae subfamily and are phylogenetically close to *Neacomys*, according to Weksler [30].

Divergence time estimates were performed using BEAST 1.8.3 [45]. For calibration, we use three calibration points (4.4 Ma corresponding to separation time estimate between *Oecomys* and *Hylaeamys* [46]; 4.5 Ma corresponding to separation between *Neacomys* and *Thalpomys*; and 5 Ma corresponding to separation between *Deltamys* and the *Neacomys/Thalpomys* clade). Uncorrelated relaxed clock was assigned to the length rates among branches and Yule prior was used for the tree. Four independent runs were made of  $20^5$  generations, showing parameters and trees every 2,500 generations. The convergence of races was evaluated in Tracer v. 1.6 [44], assuming ESS values above 200 as satisfactory. Tree's and log file's results were summarized in TreeAnnotator v. 1.8.3 and LogCombiner v. 1.8.3 [47], respectively; we discard 20% as burn-in. The tree was displayed and edited in Figtree v. 1.4.2 (<http://tree.bio.ed.ac.uk/software/figtree/>).

Estimates of ancestral areas were generated by Vicariance-Dispersion analysis (S-DIVA) implemented in RASP v. 3.2 [48]. The terminal taxa were coded correlating their ranges to areas of endemism of the Amazon (Belém, Xingu, Tapajós, Rondônia, Inambari, Guiana, Imeri and Napo) and Marajó Island [5]. The maximum number of ancestral areas chosen was three.

## Results

### Classic cytogenetics

*Neacomys* sp. A (NSP-A; Fig 1, localities 5–9) have  $2n = 58/FN = 68$  (Fig 2A) with autosomes comprising 22 acrocentric pairs (1–22) and six meta/submetacentric pairs (23–28); the X chromosome is a middle-sized submetacentric and the Y chromosome is a small-sized submetacentric. Constitutive Heterochromatin (CH) is distributed at the centromeric region of almost all autosomes. Pairs 23, 24 and 28 present large blocks of CH at a pericentromeric region. The X chromosome has a large CH block in the short arm, and the Y chromosome is almost entirely heterochromatic (Fig 2B).

*Neacomys* sp. B (NSP-B; Fig 1, localities 3 and 4) have  $2n = 54/FN = 66$  (Fig 3A) with seven meta/submetacentric autosomes pairs (1–7) and 19 acrocentric pairs (8–26). The X chromosome is a middle-sized acrocentric and the Y chromosome is small-sized. CH is distributed along the centromeric region of all autosomes and the X chromosome; the Y chromosome is almost entirely heterochromatic (Fig 3B).

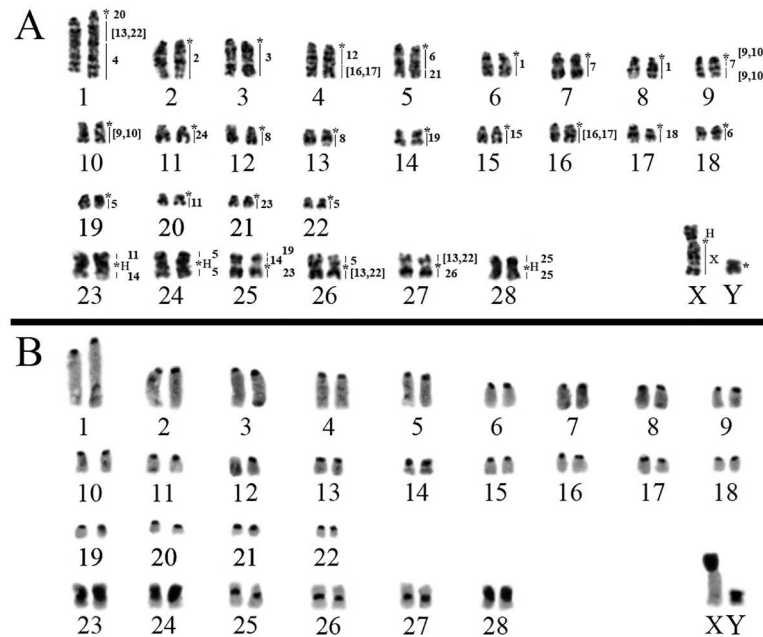


**Fig 2. *Neacomys* sp. A (2n = 58/FN = 68).** A) G-banding with chromosome painting with HME probes. B) C-banding (sequential). (H) Large block of constitutive heterochromatin. (\*) Indicates centromere.

<https://doi.org/10.1371/journal.pone.0182218.g002>

### Molecular cytogenetics

The FISH results of 24 HME whole chromosome probes [20] on two *Neacomys* species are detailed in Table 2 and Figs 2A and 3A. Centromeric (\*) and heterochromatic (H) regions do not show hybridization signals. The hybridization of each HME probe on two *Neacomys* species is detailed in S1 Fig.

***Neacomys* sp. A (NSP-A, 2n = 58 and FN = 68).** FISH with HME probes shows 40 hybridization signals in NSP-A (Fig 2A, Table 2). Eleven autosomes plus the X chromosome show conserved synteny. From those eleven, six (HME 2, 3, 15, 18, 24 and 25) hybridize whole chromosomes of NSP-A (2, 3, 15, 17, 11 and 28, respectively) and five (HME 4, 12, 20, 21 and 26) are associated with regions of other chromosomes (1q distal, 4q proximal, 1q proximal, 5q distal and 27q, respectively).

The other twelve autosomal probes show multiple signals in NSP-A, with ten (HME 1, 6, 7, 8, [9,10], 11, 14, [16,17], 19 and 23) hybridizing to two chromosomes each, where HME 1 and 8 hybridize to two whole distinct chromosomes each while the others hybridize to a chromosome and a portion of another chromosome. HME [13,22] show signals in three chromosomes and HME 5 in four different chromosomes.

Eight NSP-A pairs show chromosomal associations (to multiple HME probes): pair 1 (HME \*/20/[13,22]/4), pair 4 (HME \*/12/[16,17]), pair 5 (HME \*/6a/21), pair 9 (HME \*/[9,10]/7b/[9,10]), pair 23 (11\*/14), pair 25 (19/14\*/23), pair 26 (5\*/[13,22]) and pair 27 ([13,22]\*/26) (Table 2; Figs 2A and 4A). FISH with telomeric probes show signals only at the distal ends of chromosomes (Fig 4B).

***Neacomys* sp. B (NSP-B, 2n = 54 and FN = 66).** FISH with HME probes show 39 hybridization signals in NSP-B (Fig 3A, Table 2). Twelve autosomes plus the X chromosome show conserved synteny. From those twelve, six (HME 15, 18, 19, 24, 25 and 26) hybridized to whole chromosomes of NSP-B (9, 7, 18, 12, 13 and 17, respectively) and six (2, 3, 4, 12, 20 and 21) are

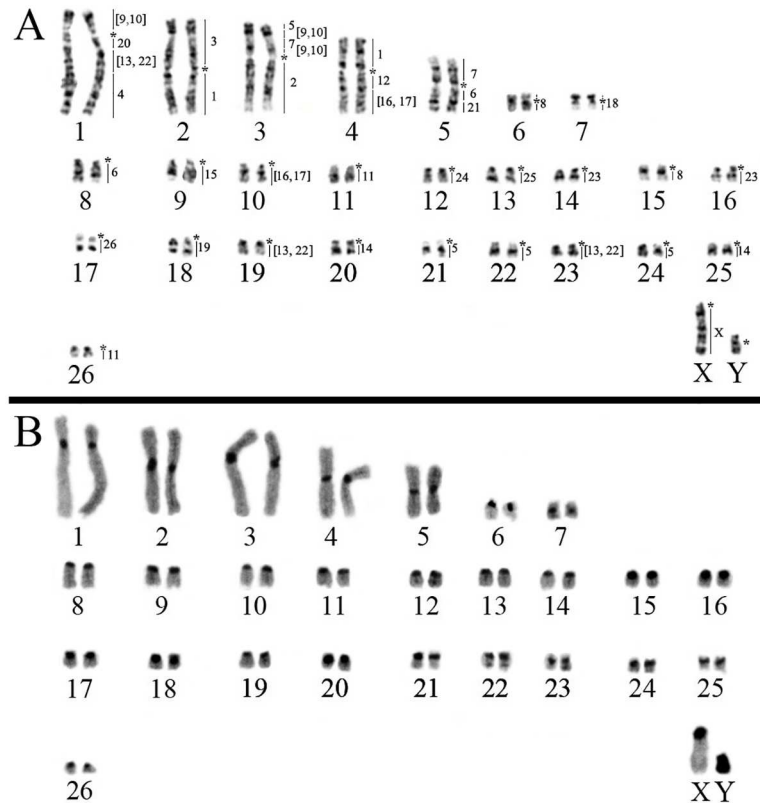


**Fig 3. *Neacomys* sp. B (2n = 54/FN = 66).** A) G-banding with chromosome painting with HME probes. B) C-banding. (\*) Indicates centromere.

<https://doi.org/10.1371/journal.pone.0182218.g003>

associated with regions of other chromosomes (NSP-B 3q, 2p, 1q distal, 4q proximal, 1q proximal and 5q distal, respectively).

The other eleven autosomal probes show multiple signals in NSP-B, with nine (HME 1, 6, 7, 8, [9,10], 11, 14, [16,17] and 23) hybridizing to two chromosomes each; HME [13,22] show signals in three chromosomes and HME 5 in four different chromosomes.

Five NSP-B pairs present chromosomal associations: pair 1 (HME [9,10]\*/20/[13,22]/4), pair 2 (HME 3\*/1b), pair 3 (HME 5/[9,10]/7b/[9,10]\*/2), pair 4 (HME 1a\*/12/[16,17]) and pair 5 (7a\*/6a/21) (Table 2; Figs 3A and 4C). FISH with telomeric probes show signals only at the distal ends of chromosomes (Fig 4D).

### Molecular phylogeny

The genus *Neacomys* was shown to be monophyletic in both analysis of maximum likelihood and Bayesian inference (Figs 5 and 6, respectively) for the concatenated mitochondrial genes (COI and Cytb; Table 3), supported by maximum values of bootstrap posterior probability. Six valid species were recovered for the clades: *N. dubosti*, *N. guianae*, *N. minutus*, *N. musseri*, *N. paracou* and *N. spinosus*. Besides, our data recovered two new clades (*Neacomys* sp. A and *Neacomys* sp. B), being monophyletic, with a high degree of divergence between them (Table 3), and other species in the *Neacomys* genus. NSP-A and NSP-B clades are described for the first time in this study.

*Neacomys* sp. samples from Marabá and Marajó Island (Fig 1, localities 1 and 2, respectively) [28] and *Neacomys* sp. A are sister lineages (Figs 5 and 6), but phylogenetically distinct.

**Table 2. Chromosomal homology among *Hylaeamys megacephalus* (HME), *Cerradomys langguthi* (CLA) [20], *Thaptomys nigrita* (TNI), *Akodon montensis* (AMO) [23], *Akodon* sp. (ASP), *Necomys lasiurus* (NLA) [22], *Neacomys* sp. A (NSP-A) and *Neacomys* sp. B (NSP-B).**

HME 2n = 54 FN = 62	TNI 2n = 52 FN = 52	AMO 2n = 24 FN = 42	ASP 2n = 10 FN = 14	NLA 2n = 34 FN = 34	CLA 2n = 46 FN = 62	NSP-A 2n = 58 FN = 68	NSP-B 2n = 54 FN = 66
1	4, 8	1q distal, 4q	1q interstitial, 2q distal	5q distal, 7	2q, 20	6, 8	2p, 4q
2	7, 12	1q interstitial, 7q	1p distal, 2q interstitial	9q interstitial, 13	10, 18, 19	2	3q
3	1 interstitial and distal	2q	2p distal	3q distal	1q interstitial, 3p	3	2p
4	13, 15	1p proximal, 5p distal	2q proximal and interstitial, 3q interstitial	1q proximal, 10q proximal, 11q distal	5, 13	1q distal	1q distal
5	2 distal, 5 proximal, 6 proximal	3q interstitial, 6p interstitial, 10	1p interstitial and proximal, 3q interstitial (2 segments)	6q distal, 12q interstitial, 14q distal	1p distal, 1q proximal, 8	19, 22, 24, 26p	3p distal, 21, 22, 24
6	3 proximal and interstitial	2p	2p interstitial	2q interstitial	4q distal	5q proximal, 18	5q proximal, 8
7	18	5q proximal, 8q	1p interstitial, 3q interstitial	1q interstitial, 4q proximal	3q interstitial	7, 9q interstitial	3p interstitial, 5p
8	6 distal	3p	3q proximal	1q interstitial	4q proximal, 7	12, 13	6, 15
[9,10]	2 proximal, 5 distal	5q, 9p	1q interstitial, 3q interstitial	1q distal, 6q proximal	2p distal, 3q distal	9q (two different segments), 10	1p, 3p interstitial (two different segments)
11	9 distal, 10 proximal	1p interstitial, 6q distal	2q interstitial, 3q distal	10q interstitial, 12q distal	11q proximal, 6	20, 23p	11, 26
12	16	1q interstitial	2q interstitial	5q proximal	2p proximal	4q proximal	4q proximal
[13,22]	9 proximal, 11 interstitial and distal, 21	3q proximal, 4p distal, 6q proximal	1q interstitial, 3q interstitial (two segments)	4q distal, 12q proximal, 14q proximal	1q (two different segments), 9	1q interstitial, 26q, 27p	1q interstitial, 19, 23
14	17 proximal, 24	6p proximal, 8p interstitial	1p interstitial, 3q interstitial	2q interstitial, 15q interstitial	1p interstitial, 21	23q, 25p proximal	20, 25
15	19	9q	1q distal	8q distal	12	15	9
[16,17]	10 distal, 22	1p distal, 3q distal	2p proximal, 2q interstitial, 3q interstitial	2q proximal, 10q distal	1q proximal, 11q distal	4q distal, 16	4q distal, 10
18	1 proximal, 23	1q proximal, 5p proximal	2p interstitial, 2q interstitial, 3q interstitial	3q proximal, 9q proximal	16	17	7
19	17 distal	8p distal, 8q proximal	1p interstitial (two segments)	15q proximal and distal	1p interstitial, 3q proximal	14, 25p distal	18
20	11 proximal	4q proximal	1q proximal and interstitial	4q interstitial	1q distal	1q proximal	1q proximal
21	3 distal	2p distal	2p interstitial	2q distal	4p, 4q interstitial	5q distal	5q distal
23	20	7p	1p interstitial	8q proximal	15	21, 25q	14, 16
24	14	6p distal	3q interstitial (two segments)	9q distal	14	11	12
25	1 proximal	2p proximal	2p interstitial, 3q interstitial	3q interstitial, 11q proximal	17	28	13
26	25	11	4	16	22	27q	17
X	X	X (Xq)	X	X	X	Xq	X
<b>Total</b>	36 signs	38 signs	45 signs	40 signs	40 signs	40 signs	39 signs

<https://doi.org/10.1371/journal.pone.0182218.t002>

The average nucleotide divergence between *Neacomys* sp. A and *Neacomys* sp. is 6.2%, while between *Neacomys* sp. B and *Neacomys* sp. is about 9.1%, and *Neacomys* sp. A and *Neacomys* sp. B is about 7.4%, both distance estimates for the concatenated mitochondrial genes (COI and Cytb; Table 3).



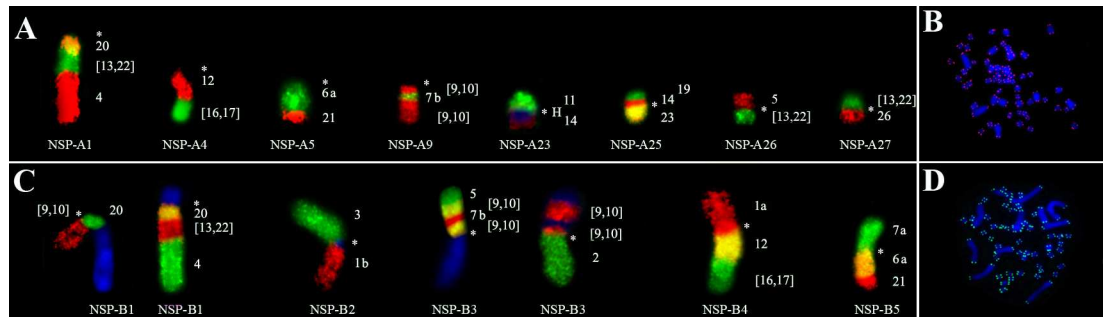


**Fig 4.** A) Chromosomal associations of *Neacomys* sp. A 1, 4, 5, 9, 23, 25, 26 and 27; B) FISH with telomeric probes in *Neacomys* sp. A. C) Chromosomal associations of *Neacomys* sp. B 1, 2, 3, 4 and 5; D) FISH with telomeric probes in *Neacomys* sp. B. (H) Indicates large block of constitutive heterochromatin. (\*) Indicates centromere.

<https://doi.org/10.1371/journal.pone.0182218.g004>

### Divergence time estimates and ancestral areas

Our divergence time estimates suggest that the diversification of species currently recognized for *Neacomys* genus occurred in the last 1.88 Ma. The last split was between *Neacomys* sp. and *Neacomys* sp. A about 0.45 Ma (Fig 7).

Our data were unable to recover some *Neacomys* ancestor nodes with high statistical support values. However, they recovered with maximum support the ancestor of *N. guianae*, *N. musseri* and *N. minutus* that occurred in current areas of Inambari and Guiana. Thus, the ancestor of *Neacomys* sp. was endemic in the Marajó Island and Xingu area.

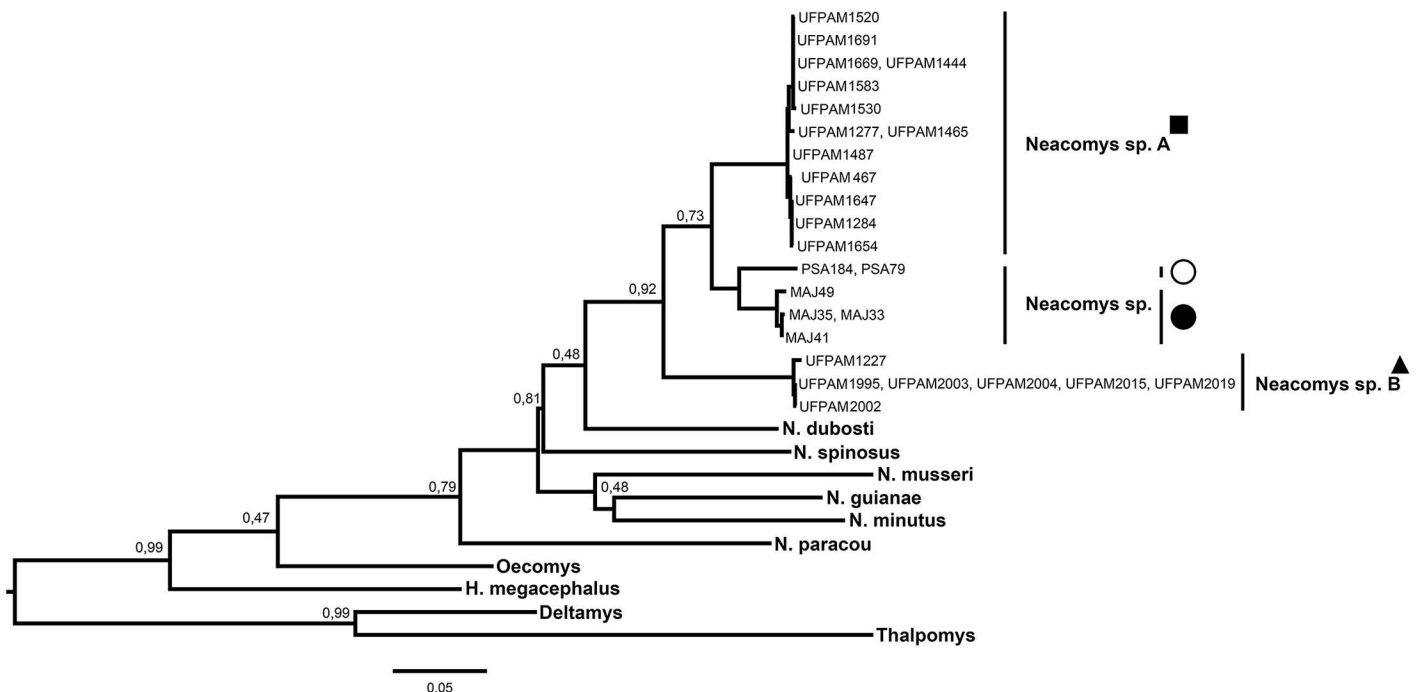


**Fig 5.** Maximum likelihood tree of specimens of *Neacomys*, based on haplotypes from 58 sequences of the concatenated mitochondrial genes (COI and Cytb). Bootstrap values are shown above the nodes. The symbols refer to species mentioned in Fig 1. Legend: black square (*Neacomys* sp. A), black triangle (*Neacomys* sp. B), white circle (*Neacomys* sp. from Marabá) and black circle (*Neacomys* sp. from Marajó island) [28].

<https://doi.org/10.1371/journal.pone.0182218.g005>

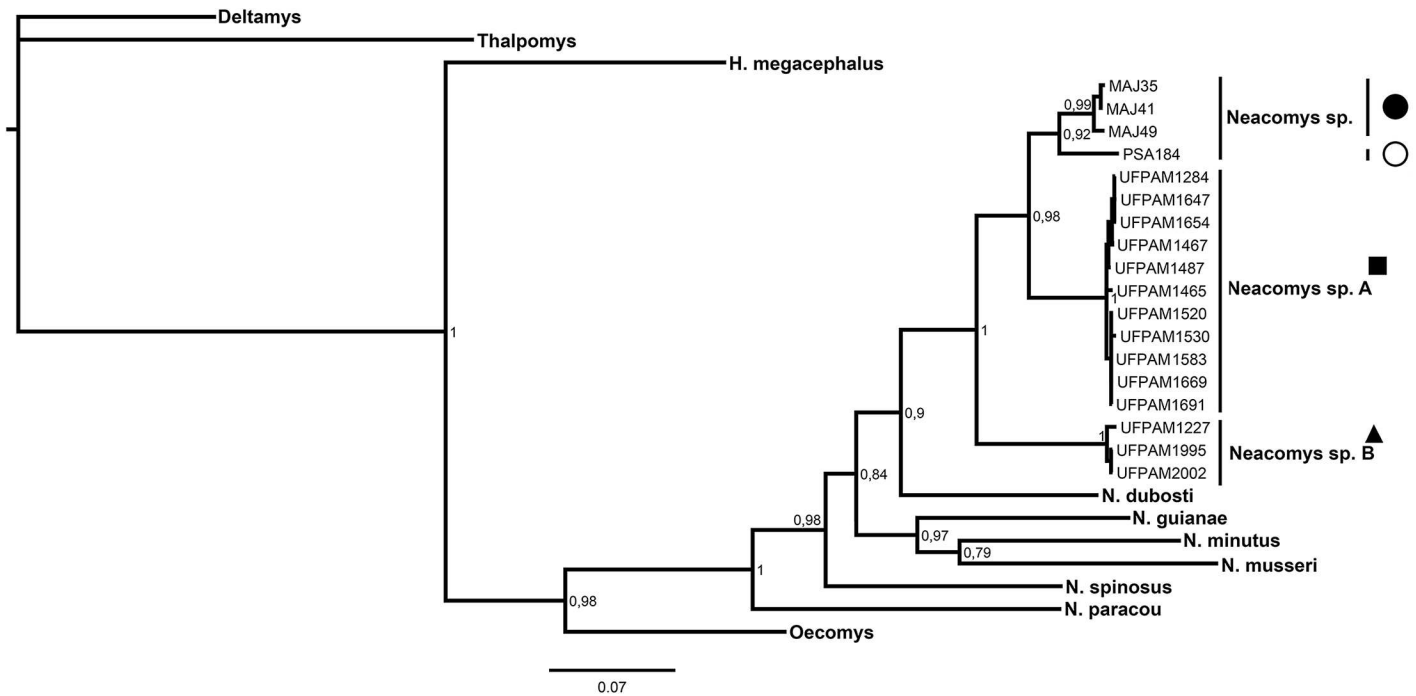


**Fig 6. Bayesian inference chronogram from BEAST estimated based on haplotypes from 58 sequences of the concatenated mitochondrial genes (COI and Cytb).** The Bayesian posterior probability (BPP) is given at each node (BS/BPP). The symbols refer to species mentioned in Fig 1. Legend: black square (*Neacomys* sp. A), black triangle (*Neacomys* sp. B), white circle (*Neacomys* sp. from Marabá) and black circle (*Neacomys* sp. from Marajó island) [28].

<https://doi.org/10.1371/journal.pone.0182218.g006>

## Discussion

### Karyotypic and phylogenetic analyses of *Neacomys*

*Neacomys* sp. A ( $2n = 58/FN = 68$ ; Fig 1, localities 5–9) presents a similar karyotype to those described by Da Silva et al. [28] for an undescribed species, identified as *Neacomys* sp., for which two karyotypes are described:  $2n = 58/FN = 64$  for Marabá, in the southeastern portion of the state of Pará (Fig 1, locality 1) and  $2n = 58/FN = 70$  for specimens from Marajó Island (Fig 1, locality 2). Comparative analysis by G- and C-banding demonstrate that the differences

**Table 3. Mean genetic distances of the concatenated mitochondrial genes Cytochrome C Oxidase—Subunit I (COI) and Cytochrome b (Cytb) according to Kimura-2 parameters among different *Neacomys* species recovered in the present study.** Values are in percentage (%).

Species	1	2	3	4	5	6	7	8	9	10	11
[1] <i>Neacomys</i> sp.											
[2] <i>Neacomys</i> sp. A	6,2										
[3] <i>Neacomys</i> sp. B	9,1	7,4									
[4] <i>N. guianae</i>	15,8	14,4	15,6								
[5] <i>N. spinosus</i>	13,7	13,5	13,0	15,7							
[6] <i>N. dubosti</i>	10,6	10,8	11,2	14,6	14,2						
[7] <i>N. paracou</i>	15,4	15,6	16,4	16,6	15,5	16,3					
[8] <i>N. musseri</i>	15,1	15,7	15,1	14,9	15,8	15,6	16,9				
[9] <i>N. minutus</i>	12,9	13,4	14,0	12,9	16,6	16,1	16,5	14,1			
[10] <i>Oecomys</i>	15,4	16,6	16,9	17,9	16,1	13,7	13,5	16,3	18,1		
[11] <i>H. megacephalus</i>	18,5	19,0	17,9	17,7	19,6	17,5	17,3	20,3	19,8	14,9	

<https://doi.org/10.1371/journal.pone.0182218.t003>

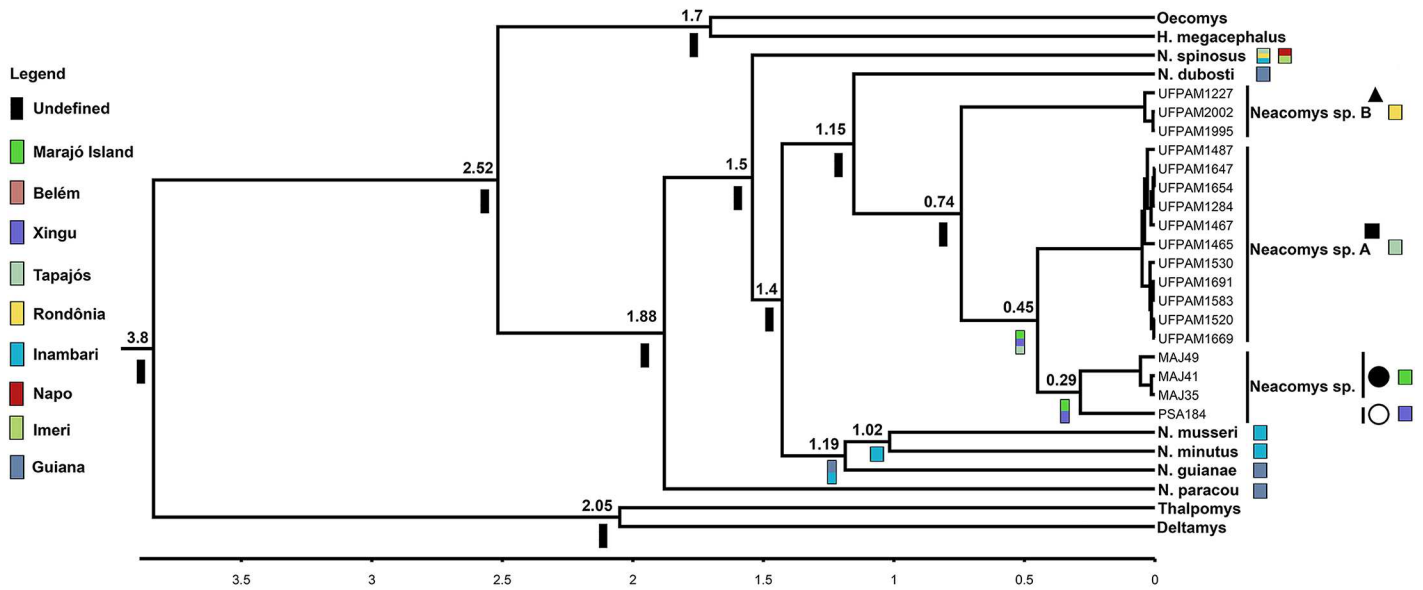


**Fig 7. Chronogram derived from a Bayesian analysis of the concatenated mitochondrial genes (COI and Cytb) of *Neacomys* genus.** The scale shows divergence times as millions of years ago (Ma). Colored bars correspond to ancestral areas recovered by Vicariance-Dispersion analysis, to Marajó island and Amazon endemic areas mentioned in Fig 1. The symbols refer to species mentioned in Fig 1. Legend: black square (*Neacomys* sp. A), black triangle (*Neacomys* sp. B), white circle (*Neacomys* sp. from Marabá) and black circle (*Neacomys* sp. from Marajó island) [28].

<https://doi.org/10.1371/journal.pone.0182218.g007>

in FN among the three karyotypes are due to differences in heterochromatic blocks, in which CH forms the short arms of some bi-armed chromosomes.

*Neacomys* sp. B ( $2n = 54/FN = 66$ ) presents a new karyotype for the genus when compared with species with  $2n$  between 56 and 64 (*N. dubosti*, *N. guianae*, *N. paracou*, *Neacomys* sp. and *N. spinosus*, Table 1). In NSP-B the bigger autosomes pairs are metacentric and submetacentric, while in other species they are medium-size acrocentrics, indicating multiple fusion/fission and/or translocation events.

According to Bradley and Baker [49] and Baker and Bradley [50], who made a meta-analysis of the genetic divergence in the Cytb gene for many groups of rodents, values of genetic divergence below 2% were present in different populations of the same species; over 5% are associated with potentially unrecognized species, and over 10% belongs to different species.

Recently, genetic approaches among eight *Neacomys* species performed by Da Silva et al. [28] found genetic divergences ranging from 10–21% (Cytb). Our results shows values ranging from 6.2–20.3% (Table 3), both are in agreement with interspecies variation values for rodents [49, 50]. Moreover, *Neacomys* sp. populations [28] from Marabá and Marajó Island (Fig 1, localities 1 and 2, respectively) constitute a single species, with an average intraspecific genetic divergence of 2% (see above).

However, *Neacomys* sp. shows a mean divergence of 6.2% for *Neacomys* sp. A and 9.1% for *Neacomys* sp. B, while *Neacomys* sp. A and *Neacomys* sp. B present a medium nucleotide divergence of 7.4% from each other in concatenated mitochondrial genes (COI and Cyt b; Table 3). These three taxa present >10% of divergence from other *Neacomys* species in both analyses.

Thus, based on the genetic species concept [49, 50] and the karyotypic and molecular data of this study, we conclude that *Neacomys* sp. A and *Neacomys* sp. B are two undescribed species within the genus and distinct from the undescribed species (*Neacomys* sp.) proposed by Da Silva et al. [28]. Moreover, these three undescribed species may represent cryptic species, which reinforces a taxonomic analysis to define their taxonomic status.

## Chromosomal rearrangements and signatures

The comparison of *Neacomys* sp. A and *Neacomys* sp. B karyotypes show that these species had a karyotypic evolutionary history that involved complex rearrangements with some chromosomal signatures that differ them from other Sigmodontinae (see below), as also many autapomorphic characteristics for each species which confirm that this genus is very diverse even in karyotypes with not very distant 2n, and they differ from one another by 11 fusion/fission events and one translocation in 16 pairs of NSP-A and 14 pairs of NSP-B, plus four pericentric inversions in four autosomal pairs, and four CH amplification events in three autosomal pairs and the X chromosome. Only eight chromosomal pairs show conserved synteny with no detectable change (Table 4, Fig 8).

**Table 4. NSP-A and NSP-B rearrangements involved.**

Rearrangement	NSP-A (2N = 58/FN = 68)	NSP-B (2N = 54/FN = 66)
Fusion/Fission	10 (*HME [9,10]) 1 (*HME 20/[13,22]/4)	1p (HME [9,10]*20/[13,22]/4) 1q (HME [9,10]*20/[13,22]/4)
Fusion/Fission	3 (*HME 3) 6 (*HME 1)	2p (HME 3*1) 2q (HME 3*1)
Fusion/Fission	22 (*HME 5) 9 (*HME [9,10]/7/[9,10]) 2 (*HME 2)	3p distal (HME 5/[9,10]/7/[9,10]*2) 3p prox +inters. (HME 5/[9,10]/7/[9,10]*2) 3q (HME 5/[9,10]/7/[9,10]*2)
Fusion/Fission	8 (*HME 1) 4 (*HME 12/[16,17])	4p (HME 1*12/[16,17]) 4q (HME 1*12/[16,17])
Fusion/Fission	7 (*HME 7) 5 (*HME 6/21)	5p (HME 7*6/21) 5q (HME 7*6/21)
Fusion/Fission	26 (HME 5*[13,22])	24 (*HME 5) + 19 (*HME [13,22])
Fusion/Fission	27 (HME [13,22]*26)	23 (HME *[13,22]) + 17 (*HME 26)
Fusion/Fission	25 (HME 19/14*23)	18qdist (*HME 19)+ 25 (*HME 14)+ 16 (*HME 23)
Translocation	14 (*HME 19)+ 25pdistal (HME 19/14*23)	18 (*HME 19)
Fusion/Fission+ H Amplification /Deletion	23 (HME 11H*H14)	11 (*HME 11) + 20 (*HME 14)
Pericentric Inversion+ H Amplification /Deletion	24 (HME 5H*H5)	22 (*HME 5)
Pericentric Inversion+ H Amplification /Deletion	28 (HME 25H*H25)	13 (*HME 25)
H Amplification /Deletion	X (H*HME X)	X (*HME X)
Pericentric Inversion	13 (*HME 8)	6 (HME 8*8)
Pericentric Inversion	17 (*HME 18)	7 (HME 18*18)
Conserved	11 (*HME 24)	12 (*HME 24)
Conserved	12 (*HME 8)	15 (*HME 8)
Conserved	15 (*HME 15)	9 (*HME 15)
Conserved	16 (*HME [16,17])	10 (*HME [16,17])
Conserved	18 (*HME 6)	8 (*HME 6)
Conserved	19 (*HME 5)	21 (*HME 5)
Conserved	21 (*HME 23)	14 (*HME 23)
Conserved	20 (*HME 11)	26 (*HME 11)

(H) Constitutive heterochromatin.

(\*) Centromere.

(p) Short arm. (q) Long arm.

(prox) Proximal.

(inters) Interstitial.

(dist) Distal.

<https://doi.org/10.1371/journal.pone.0182218.t004>

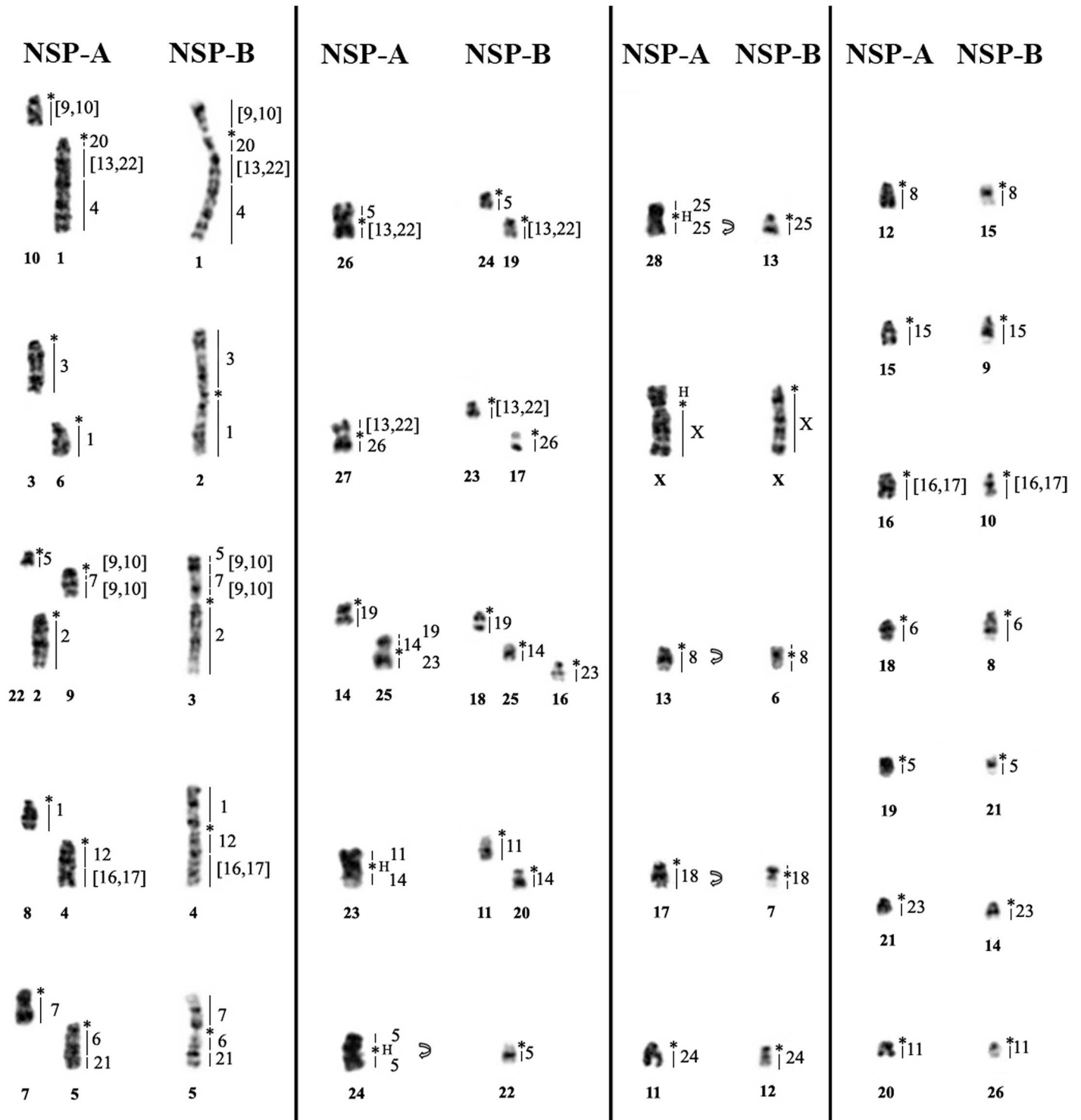


**Fig 8. Comparative analysis by G-banding and ZOO-FISH with HME whole chromosome probes [20], between *Neacomys* sp. A and *Neacomys* sp. B.** (H) Large block of constitutive heterochromatin. (\*) Indicates centromere. Curved arrow indicates pericentric inversion.

<https://doi.org/10.1371/journal.pone.0182218.g008>

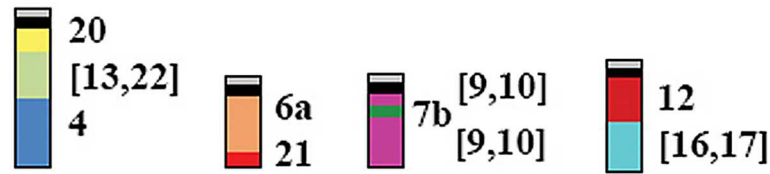


**Fig 9. Possible synapomorphic characters of *Neacomys* genus.**

<https://doi.org/10.1371/journal.pone.0182218.g009>

The absence of interstitial telomeric sequences (ITS; Fig 4B and 4D) may indicate that the rearrangements are old and that such sequences may have degenerated to the point of being undetectable by FISH [51, 52]. Alternatively, the rearrangements may have occurred without involving telomeric sequences. Similar results are described for five karyotypes of three *Neacomys* species [28].

Pereira et al. [23] have made a comparative analysis of *Akodon* sp. (ASP, Akodontini,  $2n = 10/FN = 14$ ) and *Necomys lasiurus* (NLA, Akodontini,  $2n = 34/FN = 34$ ) with *Cerradomys langguthi* (CLA, Oryzomyini,  $2n = 46/FN = 62$ ) [20], *Thaptomys nigrita* (TNI, Akodontini,  $2n = 52/FN = 52$ ) and *Akodon montensis* (AMO, Akodontini,  $2n = 24/FN = 42$ ) [22], all hybridized with HME probes. These results highlight some exclusive characters from the Akodontini tribe and some ancestral traits for the Sigmodontinae subfamily.

When we compare those authors' results with the NSP-A and NSP-B (Oryzomyini) karyotypes (Table 2), and extrapolating them using G-banding for the five karyotypes of three *Neacomys* species (*Neacomys* sp., *N. dubosti* and *N. paracou*) [28], we observe that the associations HME 20/[13,22], 6/21 and 7/[9,10], which are ancestral traits for Sigmodontinae according to Pereira et al. [23], are present also in *Neacomys*. However, these segments are rearranged in the genus and so they are synapomorphies: the first was due to a fusion with HME 4, generating HME 20/[13,22]/4; the second was due to a fission in the segment that corresponds to HME 6, generating HME 6a/21 and 6b; the third was due to a fission in the HME 7 segment, followed by a paracentric inversion, generating HME [9,10]/7b/[9,10] (Fig 9).

Although HME 1/12 and 5/[16,17] associations may be considered ancestral traits for the Sigmodontinae [23], they are absent in *Neacomys*. The association \*HME 12/[16,17] is present in *Neacomys* and is considered to be a chromosomal signature for the genus. We assume that this segment originated from a fission of HME 5/[16,17], followed by a fusion with HME [16,17] and 1/12 segments, generating HME 1/\*12/[16,17] (NSP-B 4, Fig 3); in the other species another fission occurred, generating the synapomorphy of the genus HME 12/[16,17] (Fig 9).

The association HME 19/14/19 is absent in NSP-B, but present as a derived form in NSP-A 25 (HME 19/14/\*23), with only a small segment of HME 19 in NSP-A, while the bigger fragment of HME 19 (NSP-A 14) is not associated. HME 26 is a symplesiomorphic character in NSP-B 17, while NSP-A 27 (HME [13,22]/\*26) is a derivative form. The association HME 11/[16,17] is absent in NSP-A and NSP-B.

In our comparative analysis (Table 2), we observed another trait that could belong to the hypothetical ancestral karyotype of the Sigmodontinae subfamily: HME 15 non-associated, being a symplesiomorphy in TNI 19, CLA 12, NSP-A 15 and NSP-B 7. We consider that the acrocentric HME 24 is the ancestral form, being a symplesiomorphy in TNI 14, CLA 14, NSP-A 11 and NSP-B 11, and that the metacentric form (HME) and associated (AMO 6, ASP 3, NLA 9) are derivative. We also propose other ancestral traits for the Oryzomyini tribe: HME 8 disassociated in two fragments, HME 18 non-associated and HME 25 non-associated.

## Biogeography in *Neacomys*

The geographical barrier of the Amazonian rivers [6] explains the lack of gene flow between interpluvial regions in Amazon, and confines some species to a single endemic area [5], as described for several groups of terrestrial vertebrates, including primates [53], birds [54] and rodents [55]. In the *Neacomys* genus, some species occur in more than one endemic area [2, 24–28], which is in disagreement with the pattern observed for the three undescribed species of *Neacomys*, who have isolated distributions: *Neacomys* sp. within the Marajó island and Xingu endemic area [28], *Neacomys* sp. A within the Tapajós endemic area, and *Neacomys* sp. B within the Rondônia endemic area.

In contrast to the low node support observed for *Neacomys* sp. B, our divergence time estimates (Fig 7) recovered with high statistical support indicates that the geographical area of the ancestor of *Neacomys* sp. + *Neacomys* sp. A was the current Xingu and Tapajós areas of endemism and Marajó Island, while the *Neacomys* sp. ancestor area was the current endemic area of Xingu and Marajó Island.

Our divergence time estimates (Fig 7) suggest that the diversification of *Neacomys* sp. B and *Neacomys* sp. A + *Neacomys* sp. occurred about 0.74 Ma, and the last split was between *Neacomys* sp. A and *Neacomys* sp. about 0.45 Ma. Based on speciation events in genus *Psophia* (Aves) and not on geological analyses, Ribas et al. [56] proposed that the Tapajós river drainage system was developed approximately 1.3–0.8 Ma, whereas Tocantins and Xingu rivers drainage systems were established about 0.8–0.3 Ma, acting as isolating barriers and creating the Tapajós, Xingu and Belém endemic areas.

Those divergence time estimates and diversification are within the range and in agreement with the gradient of chromosomal and molecular differentiation (see *Karyotypic and phylogenetic analyses of Neacomys* and *Chromosomal Rearrangements and Signatures*), which shows that *Neacomys* sp. [28], *Neacomys* sp. A and *Neacomys* sp. B form a monophyletic group, while the first two are sister species (Figs 5 and 6) and share more chromosomal similarities with each other than with *Neacomys* sp. B, that presents derivative chromosomal forms.

Therefore, our data supports the hypothesis that the common ancestor from these taxa was distributed through the eastern Amazon and the Tapajós and Xingu rivers formation and also Marajó Island separation of the continent act as isolating barriers to gene flow and determine the pattern of diversification of these three undescribed species. Thus, our data provide strong support for the Riverine Barrier Hypothesis [7–9].

We emphasize that NSP-A and NSP-B were collected in areas not yet related to any other previously described species or distribution areas corresponding to them, thus enlarging the geographic distribution of the *Neacomys* genus [2, 24–28], for the southwestern region of the Pará state (Brazil). The number of species within the genus and their geographical boundaries remain uncertain [2].

## Conclusions

The comparative chromosomal and molecular analyses in this study demonstrate that the Xingu and Tapajós Rivers act as geographic barriers for these three undescribed *Neacomys* species, delimiting *Neacomys* sp. distribution within the Marajó Island and Xingu endemic areas, NSP-A within the Tapajós endemic area and NSP-B within the Rondônia endemic area. In addition, we establish four synapomorphies for *Neacomys* (associations HME 20/[13,22]/4, 6a/21, [9,10]/7b/[9,10] and 12/[16,17]) and ancestral traits for the Oryzomyini tribe (HME 8a and 8b, 18 and 25) and Sigmodontinae subfamily (HME 15 and 24). It is important to continue using HME probes as taxonomic markers in other Sigmodontinae, for the definition of each tribe's chromosomal signatures and for the elucidation of taxonomic and phylogenetic relationships.

## Supporting information

**S1 Fig. Hybridization of each HME whole chromosome probe on *Neacomys* species.** A) *Neacomys* sp. A ( $2n = 58/FN = 68$ ). B) *Neacomys* sp. B ( $2n = 54/FN = 66$ ). The numbers on white circle refer to HME pair number. (TIF)

**S1 Table. List of sequenced specimens included in the molecular analysis of Cytochrome b (*Cytb*) and Cytochrome C Oxidase—Subunit I (COI) in the present study.** For each species the museum number or museum acronym, GenBank accession number and collecting locality are provided. Brazilian (BR) states are Amazonas (AM), Acre (AC) and Pará (PA). CO (Colombia), EC (Ecuador), GN (Guyana), PE (Peru), SR (Suriname) and VE (Venezuela). (\*) Sequences gently provided by J. L. Patton. (\*\*) Karyotyped specimens in this study. The numbers in parentheses refer to the localities shown in Fig 1. References are: 1. Catzeflis & Tilak (2009); 2. iBOL (2011); 3. Patton et al. (2000); 4. Hanson & Bradley (2008); 5. Borisenko et al. (2008); 6. da Silva et al. (2015); 7. Miranda et al. (2008); 8. iBOL (2012). (DOCX)

## Acknowledgments

The authors thank the Conselho Nacional de Desenvolvimento Científico e Tecnológico (CNPq), the Fundação de Amparo à Pesquisa do Pará (FAPESPA) and the Coordenação de Aperfeiçoamento de Pessoal de Nível Superior (CAPES) for financial support on projects coordinated by CY Nagamachi (Edital BIONORTE-CNPq, Proc 552032/2010-7; Edital BIONORTE-FAPESPA, ICAAF 007/2011; Edital Pró-Amazônia Proc 047/2012); the FAPESPA for financial support (Edital Vale—Proc 2010/110447) and Banco Nacional de Desenvolvimento Econômico e Social—BNDES (Operação 2.318.697.0001) on a project coordinated by JC Pieczarka; to Concremat Ambiental and Ambientare—Soluções Ambientais, for the opportunity to collect samples. Sample collections were authorized by Instituto Chico Mendes de Conservação da Biodiversidade (ICMBio) and Secretaria de Estado de Meio Ambiente do Pará (SEMA-PA).

## Author Contributions

**Conceptualization:** Cleusa Yoshiko Nagamachi.

**Data curation:** Willam Oliveira Da Silva, Julio Cesar Pieczarka, Jeferson Carneiro.

**Formal analysis:** Willam Oliveira Da Silva, Jeferson Carneiro, Cleusa Yoshiko Nagamachi.

**Funding acquisition:** Julio Cesar Pieczarka, Cleusa Yoshiko Nagamachi.

**Investigation:** Willam Oliveira Da Silva, Ana Cristina Mendes-Oliveira, Jeferson Carneiro.

**Methodology:** Julio Cesar Pieczarka, Malcolm Andrew Ferguson-Smith, Patricia Caroline Mary O'Brien, Ana Cristina Mendes-Oliveira, Cleusa Yoshiko Nagamachi.

**Project administration:** Cleusa Yoshiko Nagamachi.

**Resources:** Julio Cesar Pieczarka, Malcolm Andrew Ferguson-Smith, Patricia Caroline Mary O'Brien, Ana Cristina Mendes-Oliveira, Iracilda Sampaio, Cleusa Yoshiko Nagamachi.

**Supervision:** Cleusa Yoshiko Nagamachi.

**Visualization:** Willam Oliveira Da Silva, Iracilda Sampaio.

**Writing – original draft:** Willam Oliveira Da Silva.



**Writing – review & editing:** Julio Cesar Pieczarka, Malcolm Andrew Ferguson-Smith, Patricia Caroline Mary O'Brien, Ana Cristina Mendes-Oliveira, Iracilda Sampaio, Jeferson Carneiro, Cleusa Yoshiko Nagamachi.

## References

1. Paglia AP, Fonseca GAB, Rylands AB, Herrmann G, Aguiar LMS, Chiarello AG, et al. Lista Anotada dos Mamíferos do Brasil/Annotated Checklist of Brazilian Mammals. 2ª Edição / 2nd Edition. Occasional Papers in Conservation Biology. 2012; No. 6. Conservation International, Arlington, VA. 76 pp.
2. Patton JL, Silva MNF, Malcolm JR. Mammals of the Rio Juruá and the Evolutionary and ecological diversification of Amazonia. *Bulletin of the American Museum of Natural History*. 2000; 244: 202–292.
3. Gascon C, Malcolm JR, Patton JL, Silva MNF, Bogarti JP, Loughheed SC, Peres CA, Neckel S, Boag PT. Riverine barriers and the geographic distribution of Amazonian species. *PNAS*. 2000; vol. 97, no. 25.
4. Fernandes AM, Cohn-Haft M, Hrbek T, Farias IP. Rivers acting as barriers for BIRD dispersal in the Amazon. *Revista Brasileira de Ornitologia*. 2014; 22 (4), 361–371.
5. Silva JMC, Rylands AB, Fonseca GAB. O destino das áreas de endemismo. *MEGADIVERSIDADE*. 2005; Vol. 1, n° 1.
6. Haffer J. Hypotheses to explain the origin of species in Amazonia. *Braz. J. Biol.* 2008; 68 (4, Suppl.): 917–947.
7. Wallace A. On the monkeys of the Amazon. *Proceedings of the Zoological Society of London*. 1852; 20: 107–110.
8. Haffer J. Speciation in Amazonian forest birds. *Science*. 1969; 165:131–137. <https://doi.org/10.1126/science.165.3889.131> PMID: 17834730
9. Cracraft J. Historical biogeography and patterns of differentiation within South American birds: areas of endemism. *Ornithological Monographs*. 1985; 36: 49–84.
10. Bickford D, Lohman DJ, Sodhi NS, Ng PKL, Meier R, Winker K, et al. Cryptic species as a window on diversity and conservation. *Trends in Ecology and Evolution*. 2007; 22: 148–155. <https://doi.org/10.1016/j.tree.2006.11.004> PMID: 17129636
11. Wilson DE, Reeder DM. *Mammal Species of the World. A Taxonomic and Geographic Reference* (3rd ed), Johns Hopkins University Press. 2005; v. 2: p. 894–1531.
12. D'Elía G, Pardiñas UFJ, Teta P, Patton JL. Definition and diagnosis of a new tribe of Sigmodontinae Rodents (Cricetidae: Sigmodontinae), and a revised classification of the subfamily. *Gayana*. 2007; 71:187–194.
13. Castresana J. Cytochrome b Phylogeny and the Taxonomy of Great Apes and Mammals. *Mol. Biol. Evol.* 2001; 18(4): 465–471. PMID: 11264397
14. Ferguson-Smith MA, Yang F, O'Brien PC. Comparative mapping using chromosome sorting and painting. *ILAR J*. 1998; 39:68–76. PMID: 11528066
15. Ferguson-Smith MA, Trifonov V. Mammalian karyotype evolution. *Nat Rev Genet*. 2007; 8:950–962. <https://doi.org/10.1038/nrg2199> PMID: 18007651
16. Hass I, Sbalqueiro IJ, Müller S. Chromosomal phylogeny of four Akodontini species (Rodentia, Cricetidae) from Southern Brazil established by Zoo-FISH using *Mus musculus* (Muridae) painting probes. *Chromosome Res*. 2008; 16:75–88. <https://doi.org/10.1007/s10577-007-1211-5> PMID: 18293106
17. Swier VJ, Bradley RD, Rens W, Elder FFB, Baker RJ. Patterns of chromosomal evolution in *Sigmodon*, evidence from whole chromosome paints. *Cytogenet Genome Res*. 2009; 125:54–66. <https://doi.org/10.1159/000218747> PMID: 19617697
18. Ventura K, O'Brien PCM, Yonenaga-Yassuda Y, Ferguson-Smith MA. Chromosome homologies of the highly rearranged karyotypes of four *Akodon* species (Rodentia, Cricetidae) resolved by reciprocal chromosome painting: the evolution of the lowest diploid number in rodents. *Chromosome Res*. 2009; 17:1063–1078. <https://doi.org/10.1007/s10577-009-9083-5> PMID: 19936950
19. Hass I, Müller S, Artoni RF, Sbalqueiro IJ. Comparative chromosome maps of neotropical rodents *Necomys lasiurus* and *Thaptomys nigrita* (Cricetidae) established by ZOO-FISH. *Cytogenetic and Genome Res*. 2011; 135: 42–50.
20. Nagamachi CY, Pieczarka JC, O'Brien PCM, Pinto JA, Malcher SM, Pereira AL, et al. FISH with whole chromosome and telomeric probes demonstrates huge karyotypic reorganization with ITS between two species of Oryzomyini (Sigmodontinae, Rodentia): *Hylaeamys megacephalus* probes on *Cerradomys langguthi* karyotype. *Chromosome Research*. 2013; 21:107–119. <https://doi.org/10.1007/s10577-013-9341-4> PMID: 23494775

21. Di-Nizo CB, Ventura K, Ferguson-Smith MA, O'Brien PCM, Yonenaga-Yassuda Y, Silva MJJ. Comparative Chromosome Painting in Six Species of *Oligoryzomys* (Rodentia, Sigmodontinae) and the Karyotype Evolution of the Genus. *Plos One*. 2015; 10(2): e0117579. <https://doi.org/10.1371/journal.pone.0117579> PMID: 25658766
22. Suárez P, Nagamachi CY, Lanzone C, Malleret MM, O'Brien PCM, Ferguson-Smith MA et al. Clues on syntenic relationship among some species of Oryzomyini and Akodontini Tribes (Rodentia: Sigmodontinae). *Plos One*. 2015; 10(12): e0143482. <https://doi.org/10.1371/journal.pone.0143482> PMID: 26642204
23. Pereira AL, Malcher SM, Nagamachi CY, O'Brien PCM, Ferguson-Smith MA, Mendes-Oliveira AC et al. Extensive chromosomal reorganization among species of New World muroid rodents (Cricetidae, Sigmodontinae): Searching for phylogenetic ancestral traits. *Plos One*. 2016; 11(1): e0146179. <https://doi.org/10.1371/journal.pone.0146179> PMID: 26800516
24. Baker RJ, Koop BF, Haiduk MW. Resolving systematic relationships with g-bands: A study of five genera of South American Cricetine rodents. *Syst. Zool.* 1983; 32(4): 403–416.
25. Voss RS, Lunde DP, Simmons NB. The Mammals of Paracou, French Guiana: a neotropical lowland Rainforest fauna Part 2. Nonvolant species. *Bulletin of the American Museum of Natural History*. 2001; 263: 236 pp.
26. Redi CA, Zacharias H, Merani S, Oliveira-Miranda M, Aguilera M, Zuccotti M, et al. Genome Sizes in Afrotheria, Xenarthra, Euarchontoglires, and Laurasiatheria. *Journal of Heredity*. 2005; 96(5):485–493. <https://doi.org/10.1093/jhered/esi080> PMID: 15994420
27. Bonvicino CR, Oliveira JÁ, D'Andrea OS: Guia dos Roedores do Brasil, com chaves para gêneros baseadas em caracteres externos. Rio de Janeiro: Centro Pan-Americano de Febre Aftosa—OPAS/OMS, 2008; Série de Manuais Técnicos, 11: 120 p.
28. Da Silva WO, Pieczarka JC, Rossi RV, Schneider H, Sampaio I., Miranda CL, et al. Diversity and karyotypic evolution in the genus *Neacomys* (Rodentia, Sigmodontinae). *Cytogenetic and Genome Research*. 2015; 146: 296–305. <https://doi.org/10.1159/000441173> PMID: 26587770
29. Patton JL, Costa LP. Molecular Phylogeography and Species Limits in Rainforest Didelphid Marsupials of South America. In: Jones M, Dickman C and Archer M (eds) *Predators with Pouches: The Biology of Carnivorous Marsupials*. Sciro Publishing, Australia. 2003; pp 63–81.
30. Weksler M. Phylogenetic relationships of oryzomine rodents (Muroidea: Sigmodontinae): separate and combined analyses of morphological and molecular data. *Bulletin of the American Museum of Natural History*. 2006; 296:149p.
31. Catzeffis F, Tilak M. Molecular systematic of Neotropical spiny mice (*Neacomys*: Sigmodontinae, Rodentia) from the Guiana Region. *Mammalia*. 2009; 73: 239–247.
32. Percequillo AR, Weksler M, Costa LP. A new genus and species of rodent from the Brazilian Atlantic Forest (Rodentia: Cricetidae: Sigmodontinae: Oryzomyini), with comments on oryzomyine biogeography. *Zool J Linn Soc-Lond*. 2011; 161: 357–390.
33. Corn PS. Straight-line drift fences and pitfall traps [Chapter 7]. In: Heyer WR, Donnelly MA, McDiarmid RW, Hayek LC, Foster MS. *Measuring and monitoring biological standard methods for amphibians*. Washington, D.C.: Smithsonian Institution Press. 1994; 109–117.
34. Ford CE, Hamerton JL. A colchicine, hypotonic—citrate, squash sequence for mammalian chromosomes. *Staining Technology*. 1956; 31: 247–251.
35. Sumner AT, Evans HJ, Buckland RA. New technique for distinguishing between human chromosomes. *Nature (Lond.) New Biol*. 1971; 31: 282.
36. Sumner AT. A simple technique for demonstrating centromeric heterochromatin. *Exp Cell Res*. 1972; 75: 304–306. PMID: 4117921
37. Levan A, Fredga K, Sandberg AA. Nomenclature for centromeric position on chromosomes. *Hereditas*. 1964; 52: 201–220.
38. Ward RD, Zemlak TS, Innes BH, Last PR, Hebert PD. DNA barcoding Australia's fish species. *Philos. Trans. R. Soc. Lond. B. Biol. Sci*. 2005; 29; 360(1462):1847–57. <https://doi.org/10.1098/rstb.2005.1716> PMID: 16214743
39. Smith MF, Patton JL. Diversification of South American muroid rodents: evidence from mitochondrial DNA sequence data for the Akodontine tribe. *Biol J Linn*. 1993; Soc 50: 149–177.
40. Tanabe AS. Kakusan4 and Aminosan: two programs for comparing nonpartitioned, proportional, and separate models for combined molecular phylogenetic analyses of multilocus sequence data. *Molecular Ecology Resources*. 2011; 11: 914–921, <https://doi.org/10.1111/j.1755-0998.2011.03021.x> PMID: 21592310
41. Tamura K, Stecher G, Peterson D, Filipski A, Kumar S. MEGA 6: Molecular Evolutionary Genetics Analysis Version 6.0. *Molecular Biology and Evolution*. 2013; 30: 2725–2729. <https://doi.org/10.1093/molbev/mst197> PMID: 24132122

42. Stamatakis A. RAxML-VI-HPC: maximum likelihood-based phylogenetic analyses with thousands of taxa and mixed models. *Bioinformatics*. 2014; 22 (21), 2688–2690.
43. Ronquist F, Huelsenbeck JP. MrBayes 3: Bayesian phylogenetic inference under mixed models. *Bioinformatics*. 2003; 19 (12):1572–4. PMID: [12912839](https://pubmed.ncbi.nlm.nih.gov/12912839/)
44. Rambaut A, Suchard MA, Xie D, Drummond AJ. Tracer v1.6. 2014; <<http://beast.bio.ed.ac.uk/Tracer>>.
45. Drummond AJ, Suchard MA, Xie D, Rambaut A. Bayesian phylogenetics with beauti and the beast 1.7. *Mol Biol Evol*. 2012; 29: 1969–73. <https://doi.org/10.1093/molbev/mss075> PMID: [22367748](https://pubmed.ncbi.nlm.nih.gov/22367748/)
46. Parada A, Pardiñas UFJ, Salazar-Bravo J, D'Elía G, Palma RE. Dating an impressive Neotropical radiation: Molecular time estimates for the Sigmodontinae (Rodentia) provide insights into its historical biogeography. *Mol. Phylogenet. Evol*. 2012; <http://dx.doi.org/10.1016/j.ympev.2012.12.001>.
47. Rambaut A, Drummond AJ. TreeAnnotator version 1.8.3. 2016; <<http://beast.bio.ed.ac.uk>>.
48. Yu Y, Harris AJ, Blair C, He XJ. RASP (Reconstruct Ancestral State in Phylogenies): a tool for historical biogeography. *Molecular Phylogenetics and Evolution*. 2015; 87: 46–49. <https://doi.org/10.1016/j.ympev.2015.03.008> PMID: [25819445](https://pubmed.ncbi.nlm.nih.gov/25819445/)
49. Bradley RD, Baker RJ: A test of the genetic species concept: cytochrome-B sequences and mammals. *J Mammal*. 2001; 82: 960–973.
50. Baker RJ, Bradley RD. Speciation in mammals and the genetic species concept. *J Mammal*. 2006; 87: 643–662. <https://doi.org/10.1644/06-MAMM-F-038R2.1> PMID: [19890476](https://pubmed.ncbi.nlm.nih.gov/19890476/)
51. Zhdanova NS, Karamisheva TV, Minina J, Astakhova NM, Lansdorp P, Kammori M, et al. Unusual distribution pattern of telomeric repeats in the shrews *Sorex araneus* and *Sorex granarius*. *Chromosome Res*. 2005; 13:617–625. <https://doi.org/10.1007/s10577-005-0988-3> PMID: [16170626](https://pubmed.ncbi.nlm.nih.gov/16170626/)
52. Lin KW, Yan J. Endings in the middle: current knowledge of interstitial telomeric repeats. *Mutat Res*. 2008; 658:95–110. <https://doi.org/10.1016/j.mrrev.2007.08.006> PMID: [17921045](https://pubmed.ncbi.nlm.nih.gov/17921045/)
53. George TK, Marques SA, de Vivo M, Branch LC, Gomes N, Rodrigues R. Levantamento de mamíferos do Parna—Tapajós. *Brasil Florestal*. 1988; n° 63.
54. Oppenheimer M, Silveira LF. Taxonomy of Dark-winged Trumpeter. *Papéis Avulsos de Zoologia*. 2009; 49 (41): 547–555.
55. Rodrigues da Costa MJ, Amaral PJS, Pieczarka JC, Sampaio MI, Rossi RV, Mendes-Oliveira AC, et al. Cryptic Species in *Proechimys goeldii* (Rodentia, Echimyidae)? A Case of Molecular and Chromosomal Differentiation in Allopatric Populations. *Cytogenetic and Genome Research*. 2016; 148:199–210. <https://doi.org/10.1159/000446562> PMID: [27255109](https://pubmed.ncbi.nlm.nih.gov/27255109/)
56. Ribas CC, Aleixo A, Nogueira ACR, Miyaki CY, Cracraft J. A palaeobiogeographic model for biotic diversification within Amazonia over the past three million years. *Proc. R. Soc. B*. 2012; 279, 681–689. <https://doi.org/10.1098/rspb.2011.1120> PMID: [21795268](https://pubmed.ncbi.nlm.nih.gov/21795268/)